energies

MDPI

Article

Control Analysis with Modified LQR Method of Anti-Tank Missile with Vectorization of the Rocket Engine Thrust

Łukasz Nocoń [1,*], Marta Grzyb [1], Piotr Szmidt [1], Zbigniew Koruba [1] and Łukasz Nowakowski [2]

[1] Department of Applied Computer Science and Armament Engineering, Faculty of Mechatronics and Mechanical Engineering, Kielce University of Technology, al. Tysiąclecia Państwa Polskiego 7, 25-314 Kielce, Poland; mgrzyb@tu.kielce.pl (M.G.); pszmidt@tu.kielce.pl (P.S.); ksmzko@tu.kielce.pl (Z.K.)

[2] Department of Mechanical Engineering and Metrology, Faculty of Mechatronics and Mechanical Engineering, Kielce University of Technology, al. Tysiąclecia Państwa Polskiego 7, 25-314 Kielce, Poland; lukasn@tu.kielce.pl

* Correspondence: lnocon@tu.kielce.pl

Abstract: This article approaches the issue of the optimal control of a hypothetical anti-tank guided missile (ATGM) with an innovative rocket engine thrust vectorization system. This is a highly non-linear dynamic system; therefore, the linearization of such a mathematical model requires numerous simplifications. For this reason, the application of a classic linear-quadratic regulator (LQR) for controlling such a flying object introduces significant errors, and such a model would diverge significantly from the actual object. This research paper proposes a modified linear-quadratic regulator, which analyzes state and control matrices in flight. The state matrix is replaced by a Jacobian determinant. The ATGM autopilot, through the LQR method, determines the signals that control the control surface deflection angles and the thrust vector via calculated Jacobians. This article supplements and develops the topics addressed in the authors' previous work. Its added value includes the introduction of control in the flight direction channel and the decimation of the integration step, aimed at speeding up the computational processes of the second control loop, which is the LQR based on a linearized model.

Keywords: anti-tank missile; thrust vectoring control; optimal control; linear-quadratic regulator; control actuation system

check for updates

Citation: Nocoń, Ł.; Grzyb, M.; Szmidt, P.; Koruba, Z.; Nowakowski, Ł. Control Analysis with Modified LQR Method of Anti-Tank Missile with Vectorization of the Rocket Engine Thrust. *Energies* **2022**, *15*, 356. https://doi.org/10.3390/en15010356

Academic Editors: Paolo Mercorelli and Abdessattar Abdelkefi

Received: 13 October 2021
Accepted: 22 December 2021
Published: 4 January 2022

Publisher's Note: MDPI stays neutral with regard to jurisdictional claims in published maps and institutional affiliations.

Copyright: © 2022 by the authors. Licensee MDPI, Basel, Switzerland. This article is an open access article distributed under the terms and conditions of the Creative Commons Attribution (CC BY) license (https://creativecommons.org/licenses/by/4.0/).

1. Introduction

The development of missile control methods has long been an area of interest to scientists. The possibility of combining a missile homing system with its control system in one loop has recently drawn attention [1]. Increasing missile accuracy is the major factor that necessitates the development of engineering methods based on integration of missile subsystems [2].

Some of the control methods are based on the Riccati equation [3] and are utilized for designing non-linear control systems. The operating effectiveness of the optimal LQR control method largely depends on the elements of the Q and R weight matrix. These matrices impact the minimization of offsets generated for state variables under the influence of control signals. Combining the PID regulator tuning method with the LQR concept enables the optimization of set value tracking, with the optimal selection of setpoints for the same control object. The optimal control theory has been extended in order to tune PID regulators [4].

However, usually the Q and R weight matrices are selected via a trial-and-error method, which—apart from being time-consuming—is also onerous. Different variations (modifications) of LQR control have been used over the past decades, namely, hybrid LQR [5,6], fuzzy LQR [7,8] and switched LQR [9,10]. The author of [11] presented a description of the use of a linear-quadratic regulator (LQR) for stabilizing the characteristics

of an anti-aircraft missile and proposed an analytical method for selecting the weighting elements of the gain matrix in the feedback loop. A novel LQR tuning method using a single V parameter was proposed and tested. In [12], the linear-quadratic regulator (LQR) was involved in controlling the roll angle of a missile autopilot system. The roll controllers were represented in the second order time domain system, and the results of LQR control were distinguished from the results of sliding mode control (SMC) and fuzzy logic control (FLC). Next, the behavior of roll control systems was analyzed to decide which controller gives better performance results with respect to the desired roll angle. In [13], the authors used time as an independent variable; the motion equation of the center of mass of the target bomb was linearized, using the small disturbance method, to establish the center of mass motion of the space expressions; the LQR theory was used to design the trajectory tracking guidance law of the target projectile. The authors of [14] also used the genetic algorithm in order to optimize the weight matrices linked with the optimal regulator, while simultaneously minimizing the ITSE (Integral of Time multiplied Squared Error) index and regulator efficiency. In [15], a description was given of an application of the sliding mode control (SMC) for stabilizing the static and dynamic characteristics of an anti-aircraft missile. The solution provided an effective separation of the control process from the dynamics of the missile airframe. In the equivalent part of the stabilization system, a linear-quadratic regulator (LQR) was considered, and an analytical method of selecting the weighting elements of the gain matrix was proposed.

Owing to the progress in the development of computer systems, numerical computations enable designing ever newer LQR optimization methods and controlling multidimensional systems. In addition, LQR control has been successfully used in numerous complex situations, such as the double inverted pendulum, fuel cell systems and aircraft [16]. The LQR method belongs to the group of modern control theory methods, which analyze object model within the state space. Utilizing state space methods is relatively straightforward in the case of a multidimensional system. Taking the mathematical model into account, the selection of the control method for a tested object can be divided into a method which operates based on a mathematical model and a model-less method. The LQG optimal control method is a typical model-based method. In [17], the ship model was kept to a maneuvering trajectory through a combination of feedforward and LQG feedback control. The variances and weighting coefficients for the LQG controller were chosen systematically. On the other hand, control methods based on a fuzzy regulator and utilizing artificial neural networks are methods that do not use the object model.

LQR optimization methods have almost unlimited use. They can be successfully used in various tasks. They can be used to improve the process of making composites by infusion. In [18], authors made construction materials from laminates A, B and C with sandwich filling, using vacuum bagging, which confirmed the possibility of absorbing energy using LQR. Work is underway to optimize the selection of the appropriate layer thickness to increase the absorbed energy.

In order to choose the control method, one needs to start with analyzing the plant dynamic behavior. The dynamics of the discussed object (i.e., an anti-tank guided missile) are the change rate of its state variables, depending on its fin deflections. This relationship can, of course, be expressed in the form of a series of differential equations, also called flying object motion equations. The main goal of our article is to develop and model an innovative control actuation system for an anti-tank guided missile based on the use of the thrust vectorization, i.e., controlling the direction of the resultant thrust by deflecting the engine nozzle. The modified LQR method, which is very similar to—and at the same time an improvement on—the SDRE control method, also known in the literature, is the only way to achieve effective control of this type of innovative missile. In this paper, the equations of motion of a flying object simulate the real motion of an anti-tank missile, and the linearized form of the dynamics equations is used to calculate the control signals of the control actuation system. Control signals are determined by the modified LQR method control. While in [19], the authors the proposed dual-control missiles, which have sets of

aerodynamic fins both in front of and behind the missile center of mass, in this paper we consider a hybrid Control Actuation System (hCAS) consisting of aerodynamic surfaces and a moving missile engine nozzle, which constitutes the essence of the research for this article.

2. Model of a Hypothetical Anti-Tank Guided Missile

The controlled plant is a subsonic, hypothetical anti-tank guided short- or medium-range missile of the "fire and forget" type (Figure 1). Its in-flight control is achieved through a double control actuation system, which consists of two pairs of aerodynamic controls (rudders and elevators) in the front section of the missile and a tilting rocket engine nozzle in the rear section (Figure 2). The tilting nozzle changes the angular position of the rocket engine thrust vector resultant, relative to the missile's longitudinal axis Sx. The application of a hybrid control actuation system significantly improves missile maneuverability, as reviewed in [20].

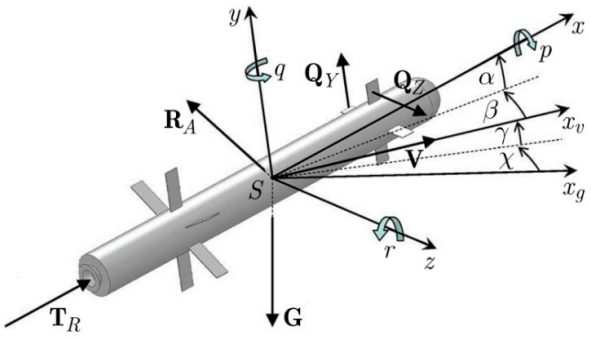

Figure 1. Force system acting on the ATGM within the gravitational field and Earth's atmosphere together with the accepted coordinate systems.

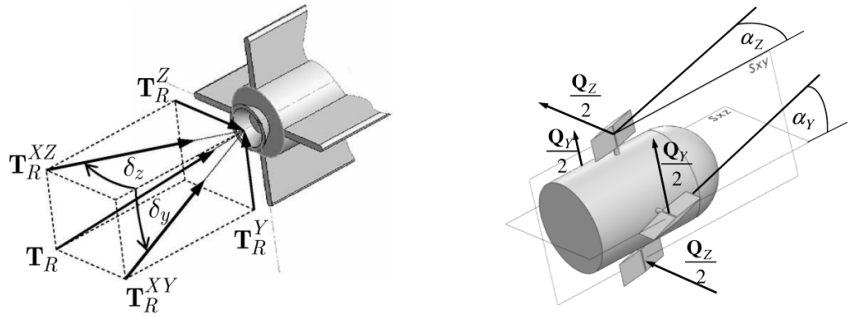

(**a**) (**b**)

Figure 2. Generation of control forces while (**a**) tilting the engine nozzle; (**b**) deflection angles of aerodynamic control surface.

Figure 1 uses the following symbols and designations: **G**—force of gravity; $\mathbf{R}_A$—vector of resultant aerodynamic forces; $\mathbf{Q}_Y$, $\mathbf{Q}_Z$—control forces; $\mathbf{T}_R$—engine thrust; **V**—vector of missile velocity; $Sx_gy_gz_g$—ground-fixed coordinate system; $Sx_vy_vz_v$—coordinate system connected with the flow; $Sxyz$—coordinate system connected with the missile; α—angle of attack; β—missile sideslip angle; γ and χ—angles of the velocity vector (flight-path angles); p, q, r—angular velocity components in the body-fixed system.

Figure 2 uses the following symbols and designations: $\mathbf{T}_R$—engine thrust; $\mathbf{T}_R^Y$—thrust projection on the vertical axis Sy; $\mathbf{T}_R^Z$—thrust projection on the horizontal axis Sz; $\mathbf{T}_R^X$—thrust projection on the longitudinal axis of the ATGM Sx; $\mathbf{T}_R^{XY}$—thrust projection on the vertical plane Sxy; $\mathbf{T}_R^{XZ}$—thrust projection on the horizontal plane Sxz; δ_z, α_Z—control angle in the horizontal plane (change yaw); δ_y, α_Y—control angle in the vertical plane (change pitch).

Deflections of the rocket engine thrust vector relative to the ATGM by δ_y, δ_z (Figure 2a) generate control forces across both planes. The flight altitude control force $\mathbf{T}_R^Y$ appears in the vertical plane, whereas the flight direction control force $\mathbf{T}_R^Z$ is generated in the plane perpendicular to the vertical plane passing through the missile's axis of symmetry [21].

The trigonometric properties indicate that: $T_R^X = T_R^{XZ}\cos\delta_z$; $T_R^Z = T_R^{XZ}\sin\delta_z$—across the horizontal plane Sxz; $T_R^X = T_R^{XY}\cos\delta_y$; $T_R^Y = T_R^{XY}\sin\delta_y$—across the vertical plane Sxy. Control forces T_R^Y and T_R^Z have been derived in detail in [21] and are equal to:

$$T_R^Y = \operatorname{sgn}(\delta_y)\left|\mathbf{T}_R^Y\right| = \operatorname{sgn}(\delta_y)\sqrt{\frac{T_R{}^2\cos^2\delta_z\cdot\sin^2\delta_y}{1-\sin^2\delta_z\cdot\sin^2\delta_y}} \approx T_R\cdot\delta_y \tag{1}$$

$$T_R^Z = \operatorname{sgn}(\delta_z)\left|\mathbf{T}_R^Z\right| = \operatorname{sgn}(\delta_z)\sqrt{\frac{T_R{}^2\cos^2\delta_y\cdot\sin^2\delta_z}{1-\sin^2\delta_z\cdot\sin^2\delta_y}} \approx T_R\cdot\delta_z \tag{2}$$

The aerodynamic controls (rudders and elevators) are located in the front of the missile (Figure 2b). A lightweight composite rudder and elevator structure [22] provides rapid response to control signals. In the case of low deflection angles of the aerodynamic controls α_Y, α_Z and subsonic velocities, the lift and lateral (control) forces Q_Y, Q_Z generated on the aerodynamic control surface adopt a simplified form (3, 4). A pair of rudders and elevators in the front part of the missile can be described by the following formulas:

$$Q_Y = 2\alpha_Y S_S \rho\frac{V^2}{2} \tag{3}$$

$$Q_Z = 2\alpha_Z S_S \rho\frac{V^2}{2} \tag{4}$$

where: S_S—area of surfaces ($S_S = 0.009\,\mathrm{m}^2$); ρ—air density ($\rho = 1.225\,\mathrm{kg/m}^3$); α_Y, α_Z—the actual deflection angles of the aerodynamic control surfaces.

The control object is guided onto a target using a thermal imaging head [23,24] or a TV head in the case of a medium-range missile, which enables the "fire and correct" mode. It is assumed that a homing head operates correctly, and the missile location data relative to the target is known. Furthermore, it is assumed that the ATGM does not rotate relative to the axis Sx.

It is assumed that the ATGM mass changes as a result of rocket engine fuel burnout. Thus, the center of mass shifts and the moments of inertia change. These changes are expressed using time-dependent linear functions (Figure 3).

Figure 3 uses the following designations:

m_0—initial mass of the ATGM = 13.287 kg;

m_1—mass of the ATGM after consumption of fuel = 8.7 kg;

x_{sm0}—initial position of the center of mass of ATGM = 0.5705 m (when viewed from the front of the ATGM);

x_{sm1}—position of the center of mass of the ATGM after consumption of fuel = 0.434 m (when viewed from the front of the ATGM);

I_{x0}—initial moment of inertia of ATGM in relation to x axis = 0.0396 kg × m^2;

I_{x1}—moment of inertia of the ATGM in relation to x axis after the consumption of fuel = 0.026 kg × m^2;

$I_{y0} = I_{z0}$—initial moment of inertia of the ATGM in relation to the transverse axis = 1.7823 kg × m^2;

$I_{y1} = I_{z1}$—moment of inertia of the ATGM in relation to the transverse axis after the consumption of fuel = 1.2078 kg × m^2;

The full spatial flight equations of dynamics for any flying object as a rigid body can be found, among others, in [25,26]. The following equations were used for this study:

$$\dot{V} = \frac{T_R}{m}\cos\alpha\cos\beta - g\sin\gamma - \lambda_x V^2 \tag{5a}$$

$$\dot{\gamma} = \frac{T_R}{mV}\sin\alpha - \frac{g}{V}\cos\gamma + \lambda_y V\alpha + \frac{Q_Y + T_R^Y}{mV} \tag{5b}$$

$$\dot{\chi} = \left(T_R\cos\alpha\sin\beta - m\lambda z V^2\beta - Q_Z - T_R^Z\right)/mV\cos\gamma \tag{5c}$$

$$\ddot{\Psi} = \left[\left(2 - \frac{I_x}{I_y}\right)\dot{\Psi}\dot{\Theta}\sin\Theta - D_1\frac{\beta}{L_P}V^2 - D_2V\dot{\beta} - D_3V\dot{\Psi} + e\frac{Q_Z}{I_y} + f\frac{T_R^Z}{I_y}\right]/\cos\Theta \tag{5d}$$

$$\ddot{\Theta} = \left(\frac{I_x}{I_z} - 1\right)\dot{\Psi}^2\sin\Theta\cos\Theta - D_1\frac{\alpha}{L_P}V^2 - D_2V\dot{\alpha} - D_3V\dot{\Theta} + e\frac{Q_Y}{I_z} + f\frac{T_R^Y}{I_z} \tag{5e}$$

where:T_R—engine thrust; $e = x_{Sm} - x_S$, $f = x_{Sm} - L_P$—distance from the center of mass of aerodynamic controls and outlet gas nozzles, correspondingly; g—acceleration due to gravity; x_S—coordinates of aerodynamic control center (when viewed from the front of ATGM); L_P—length of the ATGM body; I_x, I_y, I_z—main central moments of inertia in relation to the axes of the related system; $m = m(t)$—mass of the missile; Θ and Ψ—pitch and yaw angle of the missile body; λ_X, λ_Y,λ_Z—coefficients of aerodynamic forces; $D_i = \frac{C_i L_p}{I_z}$—relative aerodynamic factors of forces and moment; C_1—lift and drift moment factors; C_2, C_3—dumping moment factors from the ATGM body angular velocities (constants values were adopted) [27].

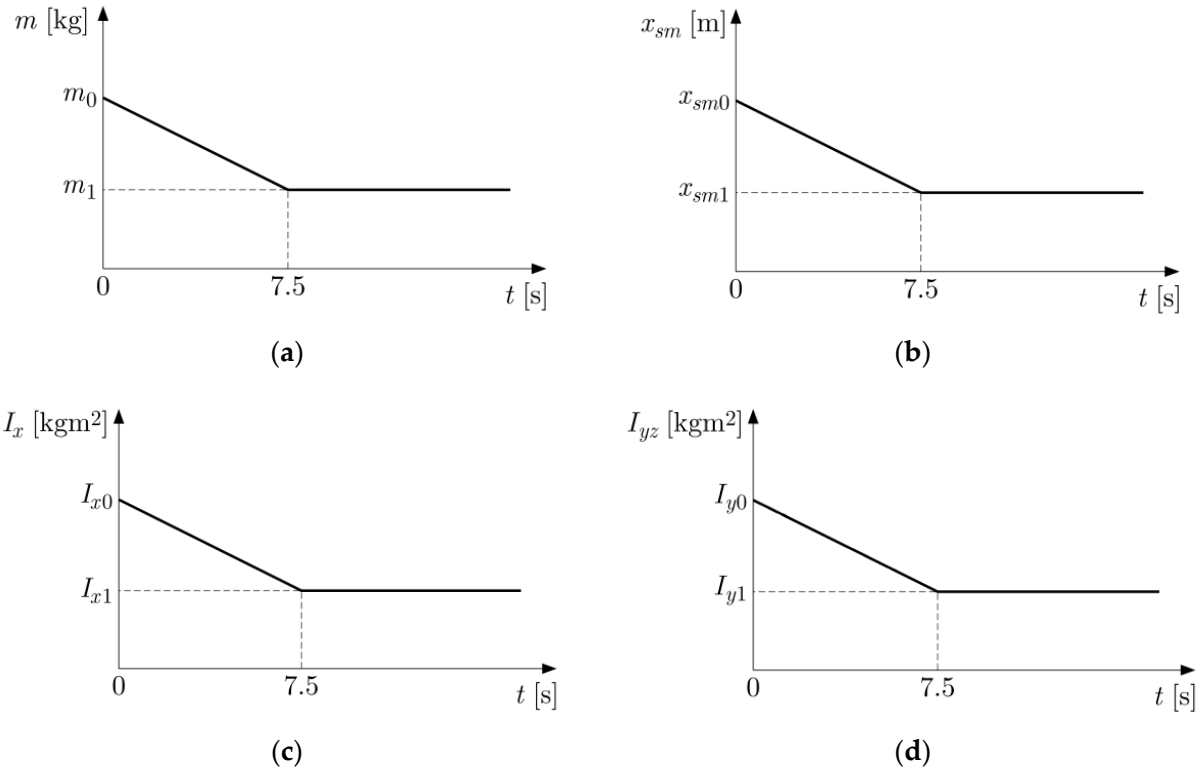

Figure 3. (**a**) Graph of mass change; (**b**) graph of the center of mass change; (**c**,**d**) graph of moments of inertia change.

The components of the angular velocity vector of a system related to the missile take the following forms (assuming that $\Phi = 0$):

$$p = \dot{\Psi}\sin\Theta \tag{6a}$$

$$q = \dot{\Psi}\cos\Theta \tag{6b}$$

$$r = \dot{\Theta} \tag{6c}$$

The projections of the linear velocity vector onto individual axes of a system related to the missile $Sxyz$ can be expressed in the form of a relationship:

$$u = V(\cos\Theta\cos\Psi\cos\gamma\cos\chi + \sin\Theta\sin\gamma + \cos\Theta\sin\Psi\cos\gamma\sin\chi) \tag{7a}$$

$$v = V(\cos\Theta\sin\gamma - \sin\Theta\sin\Psi\cos\gamma\sin\chi - \sin\Theta\cos\Psi\cos\gamma\cos\chi) \tag{7b}$$

$$w = V(\sin\Psi\cos\gamma\cos\chi - \cos\Psi\cos\gamma\sin\chi) \tag{7c}$$

The angle of attack and missile sideslip angle are determined from the following equations:

$$\alpha = \arctan\left(-\frac{v}{u}\right) \tag{8a}$$

$$\beta = \arcsin\left(\frac{w}{V}\right) \tag{8b}$$

3. The Control Algorithm in the Modified LQR Method

The general idea of programmed trajectory has been taken from [25]. Determining a programmed (preset) trajectory involves finding a third-degree polynomial function, which joins the initial point and the endpoint of a flight trajectory segment. These points are called waypoints. There can be several such trajectory segments. The last segment connects the ATGM with the target. The selection of appropriate control angles is such that the ATGM flight covers the programmed trajectory. A modified linear-quadratic regulator is used for this purpose.

ATGM flight equations of dynamics are highly non-linear. Their linearization requires major simplifications. This causes significant errors. Due to the mass changing over time (because of intensive fuel consumption) and due to the dynamic coefficients' dependance on the Mach number *Ma*, we are dealing with a non-stationary system. The authors of [21] have shown that a linear-quadratic regulator can be used to control such objects; however, when the state **A** and control **B** matrices are constant over time, the mathematical model becomes far from true. The modified LQR method removes this issue since it determines the control angles for non-linearized flight equations of dynamics (5). The control signals determined by the regulator in question are the deflection angles of the aerodynamic control surface (α_Y, α_Z) and rocket engine nozzle angles (δ_z, δ_y).

It was assumed that the aerodynamic control surface and rocket engine nozzle deflection angles have the same value but opposite directions. Therefore, we have $\alpha_Y = -\delta_y$ in the vertical plane and $\alpha_Z = -\delta_z$ in the direction control plane, which results in the following formulas:

$$Q_Y = \alpha_Y P_S,\ T_R^Y \approx -T_R \cdot \alpha_Y \tag{9a}$$

$$Q_Z = \alpha_Z P_S,\ T_R^Z \approx -T_R \cdot \alpha_Z \tag{9b}$$

$$P_S = 2S_S\rho\frac{V^2}{2} \tag{9c}$$

In a stationary state, at a given operating point, equations of dynamics take the form of a linear function. In the discussed case, the operating point of a system consists of subsequent missile flight positions when homing onto a target (executing a firing task). The operating point is updated every 100^{th} integration step, at a regulator operating frequency of 1000 Hz. As a result of decimation, the equations of dynamics are linearized every 0.1 s around the consecutive operating point. It should be emphasized that a control algorithm based on the modified LQR collects pseudo-real flight parameters from the equation of dynamics (5) to calculate control signals (Figure 4). Calculated signals control a hypothetical missile model described by Equations (5).

Equations of dynamics (5) have been reduced to the form of state Equation (10). State equations constitute a part of the regulator used to calculate the Jacobians and control matrix. The following simplifications have been introduced for the purpose of generating control signals using a modified LQR method $\alpha = \Theta - \gamma$, $\beta = \Psi - \chi$:

$$\begin{cases} \dot{V} = \frac{T_R}{m}\cos\alpha\cos\beta - g\sin\gamma - \lambda_x V^2 \\ \dot{\gamma} = \frac{T_R}{mV}\sin\alpha - \frac{g}{V}\cos\gamma + \lambda_y V\alpha + \frac{Q_Y + T_R^Y}{mV} \\ \dot{\chi} = \left(T_R\cos\alpha\sin\beta - m\lambda z V^2\beta - Q_Z - T_R^Z\right)/mV\cos\gamma \\ \omega_Y = \dot{\Psi} \\ \ddot{\Psi} = \left[\left(2 - \frac{J_x}{J_y}\right)\dot{\Psi}\dot{\Theta}\sin\Theta - D_1\frac{\beta}{L_P}V^2 - D_2 V\dot{\beta} - D_3 V\dot{\Psi} + e\frac{Q_Z}{J_y} + f\frac{T_R^Z}{J_y}\right]\Big/\cos\Theta \\ \omega_Z = \dot{\Theta} \\ \ddot{\Theta} = \left(\frac{J_x}{J_z} - 1\right)\dot{\Psi}^2\sin\Theta\cos\Theta - D_1\frac{\alpha}{L_P}V^2 - D_2 V\dot{\alpha} - D_3 V\dot{\Theta} + e\frac{Q_Y}{J_z} + f\frac{T_R^Y}{J_z} \end{cases} \quad (10)$$

The equation system (10) can be expressed in the form of a vector-matrix equation

$$\Delta\dot{\mathbf{x}}(t) = \mathbf{J}(t)\Delta\mathbf{x}(t) + \mathbf{B}\mathbf{u}(t) \quad (11)$$

where: $\dot{\mathbf{x}}(t) = \begin{bmatrix} \dot{V} & \dot{\gamma} & \dot{\chi} & \omega_Y & \ddot{\Psi} & \omega_Z & \ddot{\Theta} \end{bmatrix}^T$; $\Delta\mathbf{x}(t) = \mathbf{x}(t) - \mathbf{x}_{Set}(t)$—vector of state variables deviations from the required value; $\mathbf{x}(t) = \begin{bmatrix} V & \gamma & \chi & \Psi & \dot{\Psi} & \Theta & \dot{\Theta} \end{bmatrix}^T$—vector of actual state variables; $\mathbf{x}_{Set}(t)$—vector of state variables at work point, i.e., vector of required values of state variables; $\mathbf{u}(t) = [\alpha_Y, \alpha_Z]^T$—vector of forcing (control of) the system; **J**—Jacobian, system state matrix, calculated within each sample time; **B**—control matrix.

$$\mathbf{B} = \begin{bmatrix} 0 & 0 \\ \frac{P_S - T_R}{mV} & 0 \\ 0 & \frac{(-P_S + T_R)}{mV\cos\gamma} \\ 0 & 0 \\ 0 & \frac{D_2(T_R - P_S)}{m\cos\lambda} + \frac{eP_S - fT_R}{J_y\cos\Theta} \\ 0 & 0 \\ \frac{D_2(P_S - T_R)}{m} + \frac{eP_S - fT_R}{J_y} & 0 \end{bmatrix} \quad (12)$$

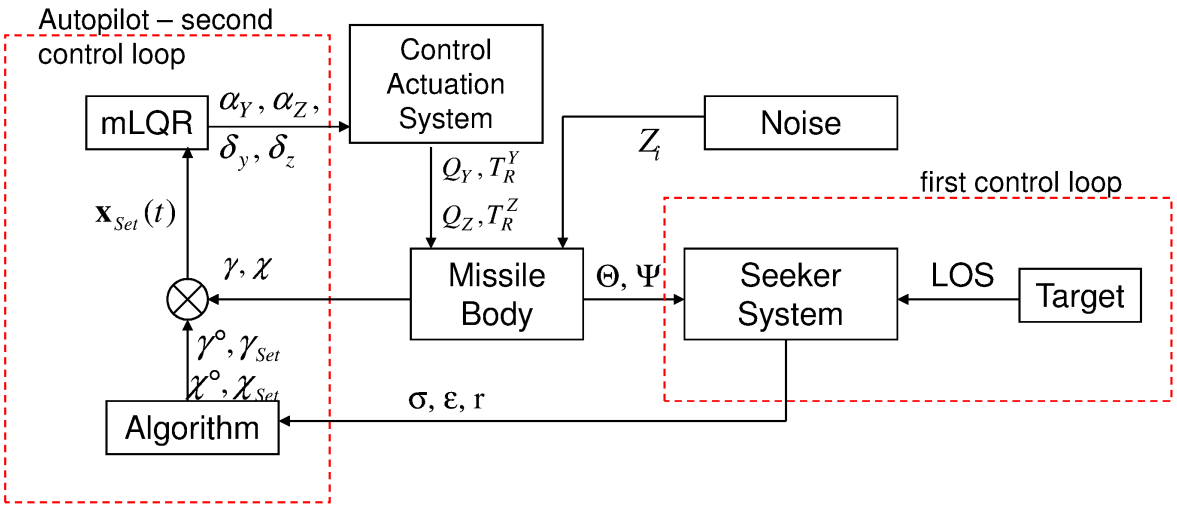

Figure 4. Scheme of controlling a hypothetical missile using a modified LQR method.

It should be noted that calculating the Jacobian determinants at any moment in time enables the shifting of the operating point to the current ATGM location. However, such a solution consumes a large share of the autopilot's computing power, which can result in reduced operating effectiveness. This is why the Jacobian **J**, control matrix **B** and operating point are updated periodically (i.e., 0.1 s) during the tests. The data needed for LQR method

control are taken directly from the mathematical model expressed in the form of equations of dynamics, described by the formulas (5). Via a new Jacobian **J** and control matrix **B**, the gain matrix **K** is determined for the LQR.

Let us express the Jacobian of the system described by Equation (10) in the following form:

$$\mathbf{J}(t) = \left[\begin{array}{ccccccc} \frac{\partial \dot{V}}{\partial V} & \frac{\partial \dot{V}}{\partial \gamma} & \frac{\partial \dot{V}}{\partial \chi} & \frac{\partial \dot{V}}{\partial \Psi} & \frac{\partial \dot{V}}{\partial \dot{\Psi}} & \frac{\partial \dot{V}}{\partial \Theta} & \frac{\partial \dot{V}}{\partial \dot{\Theta}} \\ \frac{\partial \dot{\gamma}}{\partial V} & \frac{\partial \dot{\gamma}}{\partial \gamma} & \frac{\partial \dot{\gamma}}{\partial \chi} & \frac{\partial \dot{\gamma}}{\partial \Psi} & \frac{\partial \dot{\gamma}}{\partial \dot{\Psi}} & \frac{\partial \dot{\gamma}}{\partial \Theta} & \frac{\partial \dot{\gamma}}{\partial \dot{\Theta}} \\ \frac{\partial \dot{\chi}}{\partial V} & \frac{\partial \dot{\chi}}{\partial \gamma} & \frac{\partial \dot{\chi}}{\partial \chi} & \frac{\partial \dot{\chi}}{\partial \Psi} & \frac{\partial \dot{\chi}}{\partial \dot{\Psi}} & \frac{\partial \dot{\chi}}{\partial \Theta} & \frac{\partial \dot{\chi}}{\partial \dot{\Theta}} \\ \frac{\partial \omega_Y}{\partial V} & \frac{\partial \omega_Y}{\partial \gamma} & \frac{\partial \omega_Y}{\partial \chi} & \frac{\partial \omega_Y}{\partial \Psi} & \frac{\partial \omega_Y}{\partial \dot{\Psi}} & \frac{\partial \omega_Y}{\partial \Theta} & \frac{\partial \omega_Y}{\partial \dot{\Theta}} \\ \frac{\partial \ddot{\Psi}}{\partial V} & \frac{\partial \ddot{\Psi}}{\partial \gamma} & \frac{\partial \ddot{\Psi}}{\partial \chi} & \frac{\partial \ddot{\Psi}}{\partial \Psi} & \frac{\partial \ddot{\Psi}}{\partial \dot{\Psi}} & \frac{\partial \ddot{\Psi}}{\partial \Theta} & \frac{\partial \ddot{\Psi}}{\partial \dot{\Theta}} \\ \frac{\partial \omega_Z}{\partial V} & \frac{\partial \omega_Z}{\partial \gamma} & \frac{\partial \omega_Z}{\partial \chi} & \frac{\partial \omega_Z}{\partial \Psi} & \frac{\partial \omega_Z}{\partial \dot{\Psi}} & \frac{\partial \omega_Z}{\partial \Theta} & \frac{\partial \omega_Z}{\partial \dot{\Theta}} \\ \frac{\partial \ddot{\Theta}}{\partial V} & \frac{\partial \ddot{\Theta}}{\partial \gamma} & \frac{\partial \ddot{\Theta}}{\partial \chi} & \frac{\partial \ddot{\Theta}}{\partial \Psi} & \frac{\partial \ddot{\Theta}}{\partial \dot{\Psi}} & \frac{\partial \ddot{\Theta}}{\partial \Theta} & \frac{\partial \ddot{\Theta}}{\partial \dot{\Theta}} \end{array} \right] \Bigg|_{X_0} \tag{13}$$

The matrix **J** is a Jacobian of a system of Equation (10) and consists of partial derivatives calculated for each operating point $x_0 \left(V_0 \, \gamma_0 \, \chi_0 \, \Psi_0 \, \dot{\Psi}_0 \, \Theta_0 \, \dot{\Theta}_0 \right)$.

The right of control $\mathbf{u} = \mathbf{u}(t)$ was determined and minimizes the quadratic quality index:

$$J = \frac{1}{2} \int_0^{tk} \mathbf{x}^T(t) \mathbf{Q} \mathbf{x}(t) + \mathbf{u}^T(t) \mathbf{R} \mathbf{u}(t) dt \tag{14}$$

where: **Q**—positively semi-definite symmetric matrix; **R**—positively definite symmetric matrix; t_k—simulation end time.

In essence, we are dealing with an LQR finite horizon problem. However, the cost function (14) is written without the third part responsible for the state deviation at termination time. This is because it is much more important to maintain the control accuracy for the entire time interval of a given linearization of the system. Moreover, the problem can be solved using the algebraic Riccati equation instead of the Riccati differential equation, which saves computing power in embedded systems. For research and simulation purposes, the lqr function from the MATLAB Control System Toolbox [28] was used.

The LQR gain matrix was determined based on dynamic equations, and it allows us to minimize the quadratic quality index (14):

$$\mathbf{K} = \mathbf{R}^{-1} \mathbf{B}^T \mathbf{S} \tag{15}$$

The minimization process involves solving an algebraic Riccati equation, which can be determined using the lqr function in Matlab [29].

Matrices **Q**, **R** are selected for two time intervals. The first time interval is the time when the launch motor is on ($0 \leq t < 0.5$ s) and the thrust is 4.3 kN. The second interval is when the main engine is on ($0.5 \leq t < 7.5$ s), the thrust of which is 280 N. The stability of the control system when switching between different gains K is ensured by appropriate software limitations. Appropriate limitations simulating the real movement of the actuators are introduced in the simulation. The first limitation concerns the deflection angles of the aerodynamic control surfaces (from −16 deg to 16 deg). The second limitation concerns the velocity of the actuators. The third is the limited forces generated by the control actuation systems. The operating stability of the control system used is ensured by the selection of LQR regulator settings, which are responsible for the determination of the **Q** and **R** weights matrices. As is well known, the LQR algorithm does not have a universal method for selecting the above parameters, and they are usually iteratively selected. In this paper, when selecting the initial values of **Q** and **R** matrices, the authors used the Bryson [30] rule, which allowed for determining the selection of the following input parameters:

$$\mathbf{Q}_{ii} = \frac{1}{x_{ii}^2} \tag{16a}$$

$$\mathbf{R}_{ii} = \frac{1}{u_{ii}^2} \tag{16b}$$

where: i—another element of the state vector; x_{ii}—the maximum values for individual elements of the state vector x; u_{ii}—the maximum control moments. The maximum operating parameters of the rocket missile were determined using the Lapunov method, and they are, respectively:

$$\mathbf{Q}_{t<0.5\text{ s}} = \begin{bmatrix} 0.474 & 0 & 0 & 0 & 0 & 0 & 0 \\ 0 & 3.6 & 0 & 0 & 0 & 0 & 0 \\ 0 & 0 & 1.6 & 0 & 0 & 0 & 0 \\ 0 & 0 & 0 & 0.6 & 0 & 0 & 0 \\ 0 & 0 & 0 & 0 & 0.004 & 0 & 0 \\ 0 & 0 & 0 & 0 & 0 & 1.6 & 0 \\ 0 & 0 & 0 & 0 & 0 & 0 & 0.0021 \end{bmatrix} \tag{17a}$$

$$\mathbf{R}_{t<0.5\text{ s}} = \begin{bmatrix} 0.382 & 0 \\ 0 & 0.58 \end{bmatrix} \tag{17b}$$

$$\mathbf{Q}_{0.5\text{ s}\leq t} = \begin{bmatrix} 0.01 & 0 & 0 & 0 & 0 & 0 & 0 \\ 0 & 0.91 & 0 & 0 & 0 & 0 & 0 \\ 0 & 0 & 0.71 & 0 & 0 & 0 & 0 \\ 0 & 0 & 0 & 0.01 & 0 & 0 & 0 \\ 0 & 0 & 0 & 0 & 0.04 & 0 & 0 \\ 0 & 0 & 0 & 0 & 0 & 0.001 & 0 \\ 0 & 0 & 0 & 0 & 0 & 0 & 0.00151 \end{bmatrix} \tag{17c}$$

$$\mathbf{R}_{0.5\text{ s}\leq t} = \begin{bmatrix} 0.391 & 0 \\ 0 & 0.84 \end{bmatrix} \tag{17d}$$

It was assumed that the linear system is in a state of equilibrium. The objective of control was to maintain control at a preset operating point, despite the disturbances affecting it. In this case, the ATGM moves, and the operating point is not constant. The state of equilibrium depends on the offset $\mathbf{x}(t) - \mathbf{x}_{Set}(t)$. Optimal control takes the form:

$$\mathbf{u}(t) = -\mathbf{K}(\mathbf{x}(t) - \mathbf{x}_{Set}(t)) \tag{18}$$

After substituting Equations (18) to (11), we get:

$$\Delta\dot{\mathbf{x}}(t) = (\mathbf{J} - \mathbf{B}\mathbf{K})(\mathbf{x}(t) - \mathbf{x}_{Set}(t)) \tag{19}$$

The vector of set state variables $\mathbf{x}_{Set}(t) = \begin{bmatrix} V_0 & \gamma^\circ + \gamma_{Set} & \chi^\circ + \chi_{Set} & \Psi_0 & \dot{\Psi}_0 & \Theta_0 & \dot{\Theta}_0 \end{bmatrix}^T$ was derived from data calculated based on the programmed trajectory.

The programmed trajectory of flight within the vertical and horizontal planes are third-degree polynomials y_{Set}, z_{Set}, used to calculate the set angle of control for the altitude and flight direction γ_{Set}, χ_{Set}:

$$y_{Set} = a_y x^3 + b_y x^2 + c_y x + d_y \tag{20a}$$

$$z_{Set} = a_z x^3 + b_z x^2 + c_z x + d_z \tag{20b}$$

$$\gamma_{Set} = arctg\left(3a_y x^2 + 2b_y x + c_y\right) \tag{20c}$$

$$\chi_{Set} = arctg\left(3a_z x^2 + 2b_z x + c_z\right) \tag{20d}$$

In addition, the set variable vector was expanded with an angular correction of altitude and direction. The angular position correction results from trigonometric properties. It has the following form:

$$\gamma^\circ = arctg\left(\frac{\Delta y}{\Delta x}\cos\gamma_{Set}\right) \tag{21a}$$

$$\chi^\circ = arctg\left(\frac{\Delta z}{\Delta x}\cos\chi_{Set}\right) \tag{21b}$$

where: $a_y, b_y, c_y, a_z, b_z, c_z$—polynomial coefficients calculated according to the control algorithm [23]; $\Delta y = y_{Set} - y$, $\Delta z = z_{Set} - z$; y_{Set}, z_{Set}—programmed trajectory coordinates; y, z—real ATGM coordinates; Δx—projected distance necessary to correct the ATGM flight—assumed as:$\Delta x = 10$ m.

4. Results

The simulation was conducted for a hypothetical missile described by equations of dynamics (5) and controlled using a modified LQR. The control actuation system is a double system consisting of aerodynamic controls (rudders and elevators) in the front section of the missile and variable rocket engine thrust geometry. The geometric and mass properties of the ATGM and other parameters are selected as follows:

$L_p = 1.2$ m; $x_s = 0.2$ m; $D_1 = 0.0481$ 1/m; $D_2 = 0.0821$ 1/m; $D_3 = 0.00041$ 1/m; $\lambda_x = 0.000171$ 1/m; $\lambda_y = \lambda_z = 0.051$ 1/m. The simulations present the results obtained for the Jacobian matrix updated for every 0.1 s.

Numerical simulations were conducted for a hypothetical missile. The following numerical values were used: the starting point of the ATGM is located at the beginning of the coordinate system $Ox_g y_g z_g$, the initial velocity of the ATGM $V_0 = 50$ m/s, sample time $dt = 0.001$ s, and the pitch and yaw angles of starting $\Theta = 0$ deg, $\Psi = 0$ deg.

Matlab software was used to simulate and validate the results.

4.1. The First Simulation

The simulation results presented in Figures 5–11 concern the missile flight for the following parameters: starting target position: $x_{t0} = 1200$ m, $y_{t0} = 0$ m, $z_{t0} = 0$ m; angle of the missile launch: $\gamma_{m0} = 0$ deg, $\chi_{m0} = 0$ deg; starting angle of pitch and yaw of the target velocity vector: $\gamma_{t0} = 0$ deg, $\chi_{t0} = 0$ deg; target velocity: $V_t = 30$ m/s. Missile passing through two waypoints: P_1 (400; 30; −30) and P_2 (750; 4; 10).

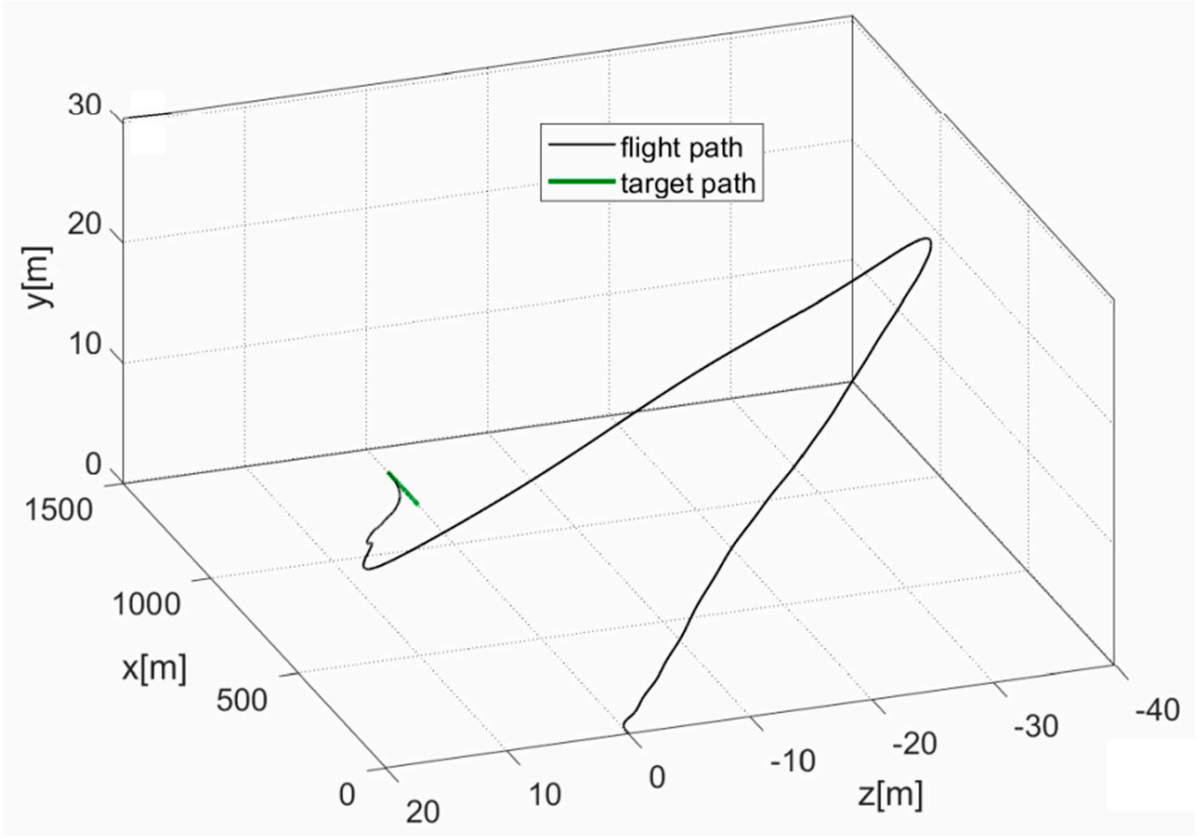

Figure 5. The performed trajectory in the 3D space.

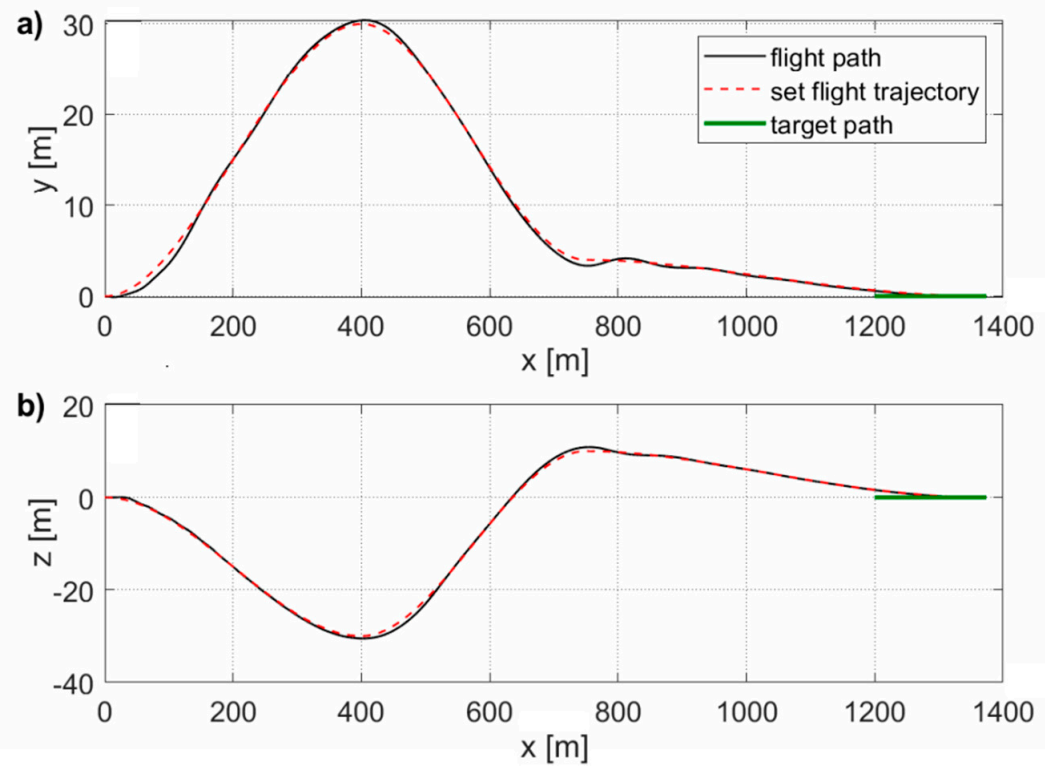

Figure 6. The performed and set flight trajectory in (**a**) the vertical plane; (**b**) the horizontal plane.

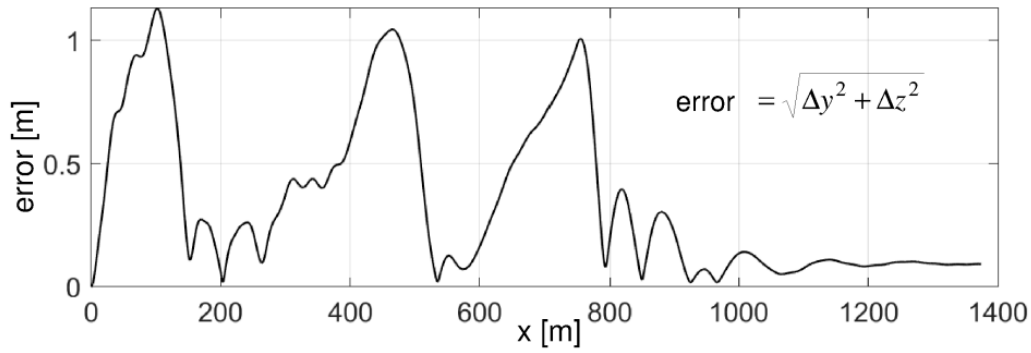

Figure 7. The control errors between the performed and set flight trajectory.

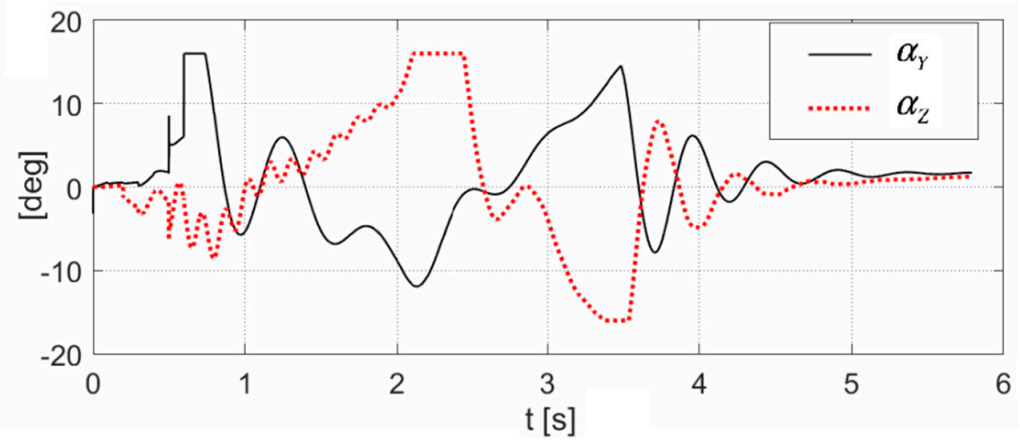

Figure 8. The performed angles of the flight control in the channel of altitude and direction.

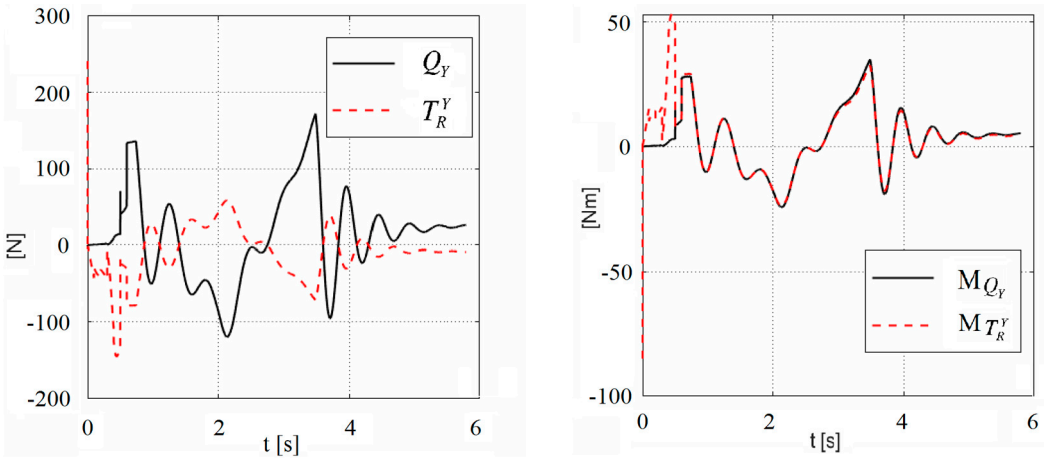

(**a**) (**b**)

Figure 9. The performed control forces (**a**) and moments (**b**) of the anti-tank guided missile flight in the vertical plane.

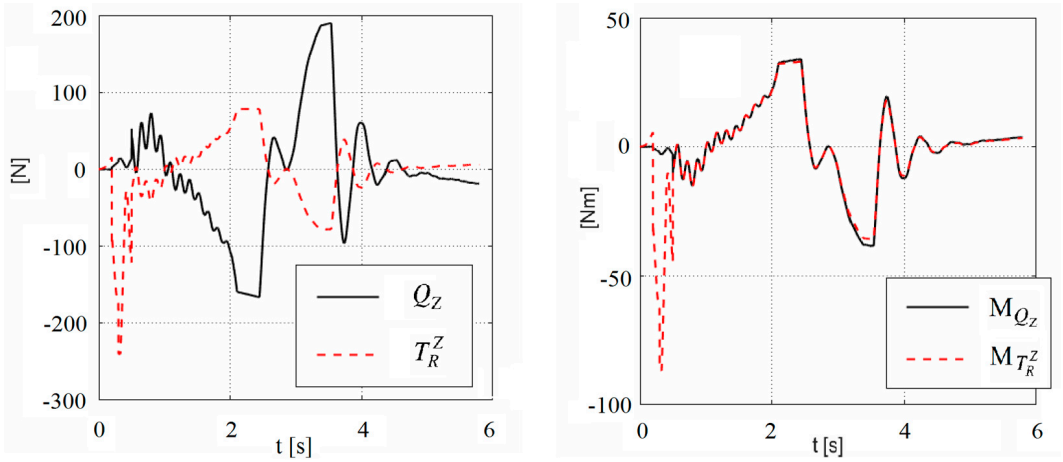

(**a**) (**b**)

Figure 10. The performed control forces (**a**) and moments (**b**) of the anti-tank guided missile flight in the horizontal plane.

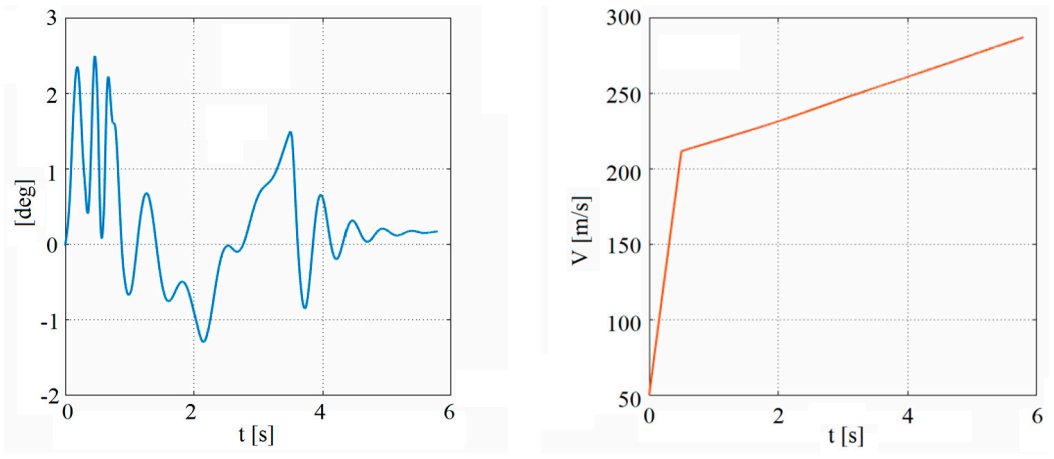

(a) **(b)**

Figure 11. Implemented angle of attack α (**a**) and velocity of the ATGM (**b**) in function of time.

4.2. The Second Simulation

The simulation results presented in Figures 12–18 concern the missile flight for the following parameters: starting target position: x_{t0} = 2000 m, y_{t0} = 5 m, z_{t0} = −1 m; angle of the missile launch: $\gamma_{m0} = 0$ deg, $\chi_{m0} = 0$ deg; starting angle of pitch and yaw of the target velocity vector: $\gamma_{t0} = 5$ deg, $\chi_{t0} = 10$ deg; target velocity: V_t = 20 m/s. Missile passing through four points: P_1 (400; 30; −30), P_2 (700; 4; 0), P_3 (1100; 20; 10), P_4 (1700; 20; −20).

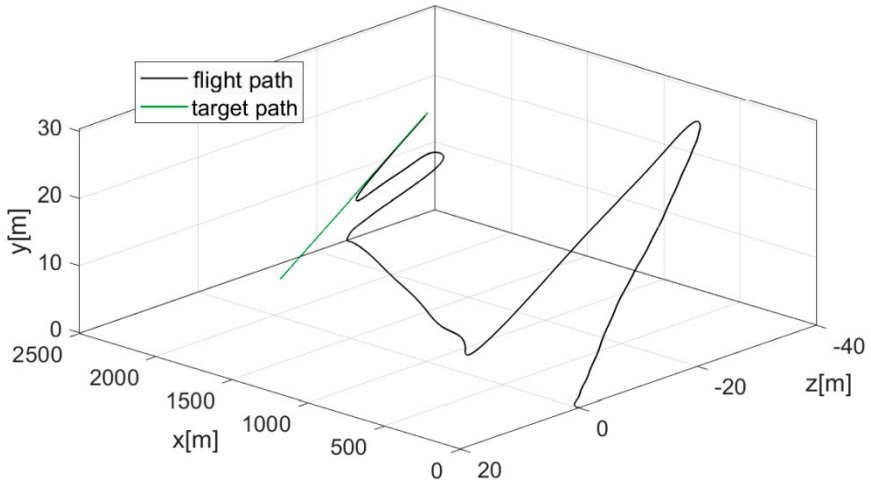

Figure 12. The performed trajectory in the 3D space.

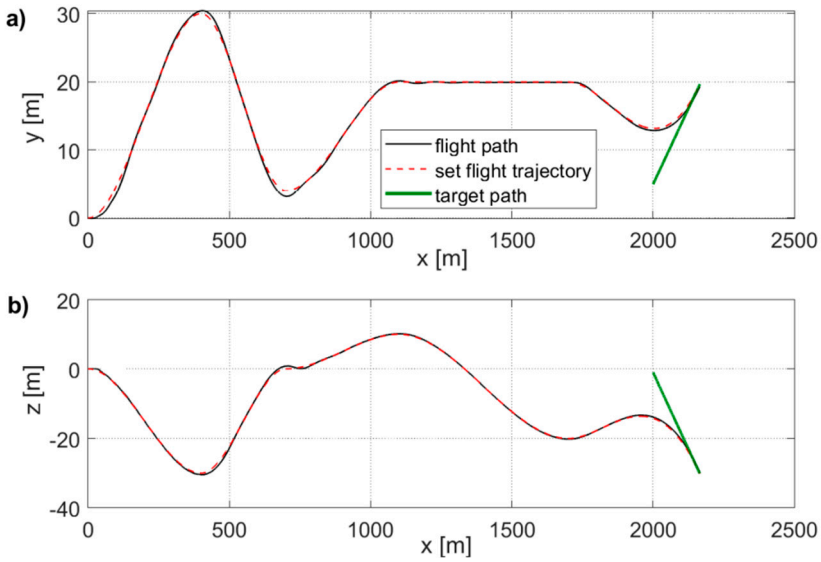

Figure 13. The performed and desired flight trajectory in (**a**) the vertical plane; (**b**) the horizontal plane.

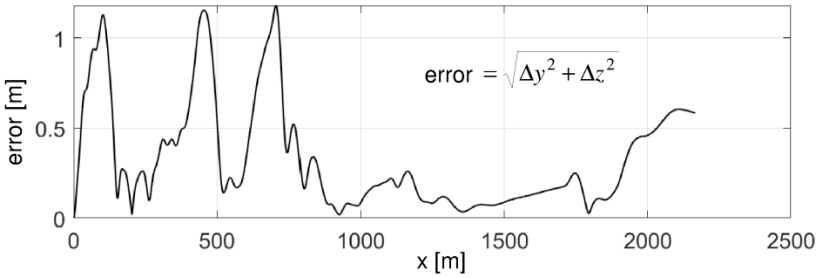

Figure 14. The control errors between the performed and set flight trajectory.

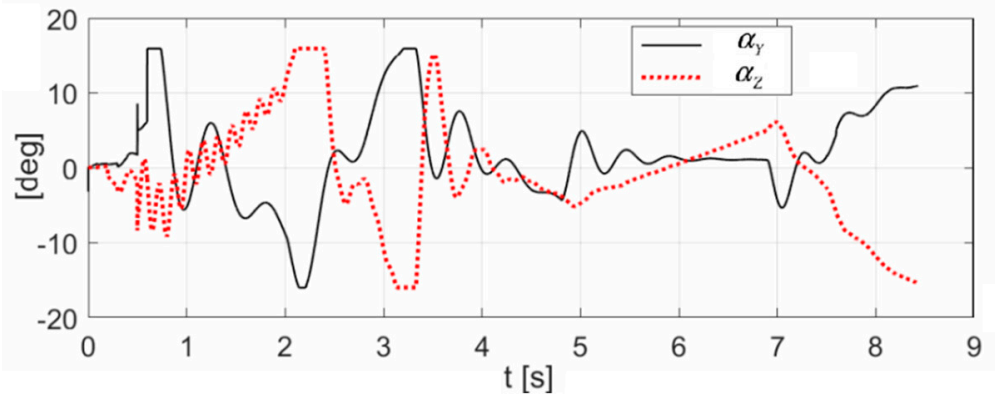

Figure 15. The performed angles of the flight control in the channel of altitude and direction.

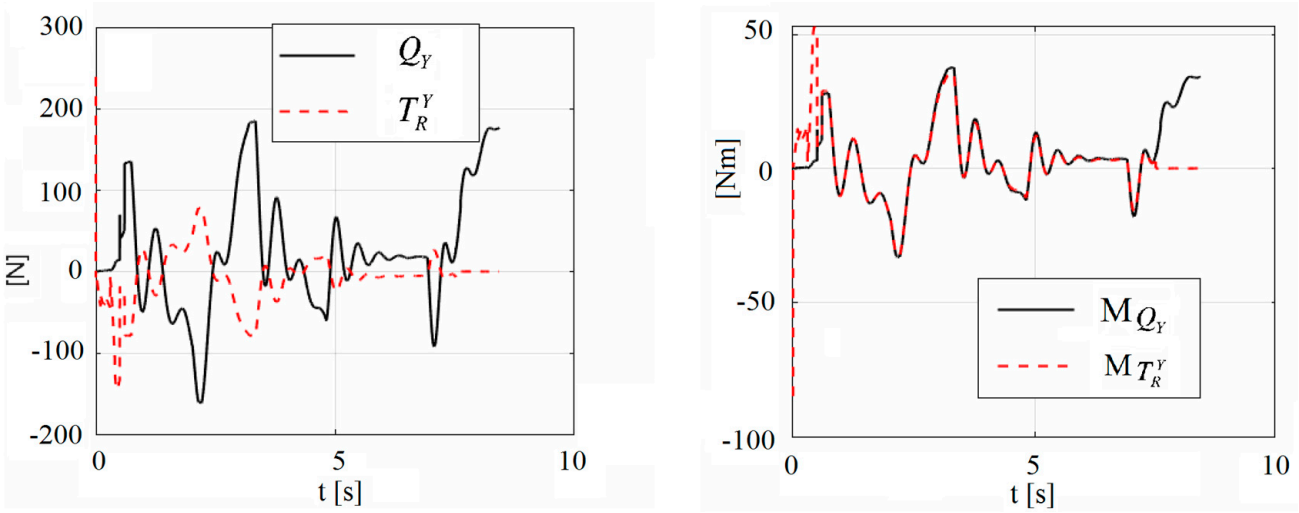

(a) **(b)**

Figure 16. The performed control forces (**a**) and moments (**b**) of the anti-tank guided missile flight in the vertical plane.

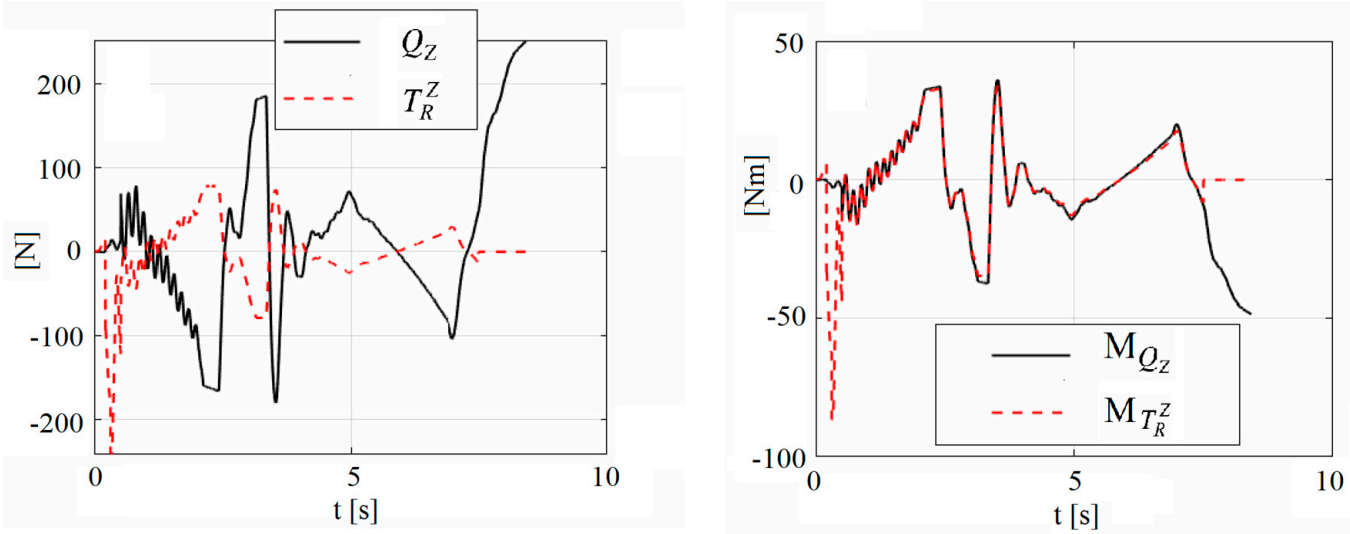

(a) **(b)**

Figure 17. The performed control forces (**a**) and moments (**b**) of the anti-tank guided missile flight in the horizontal plane.

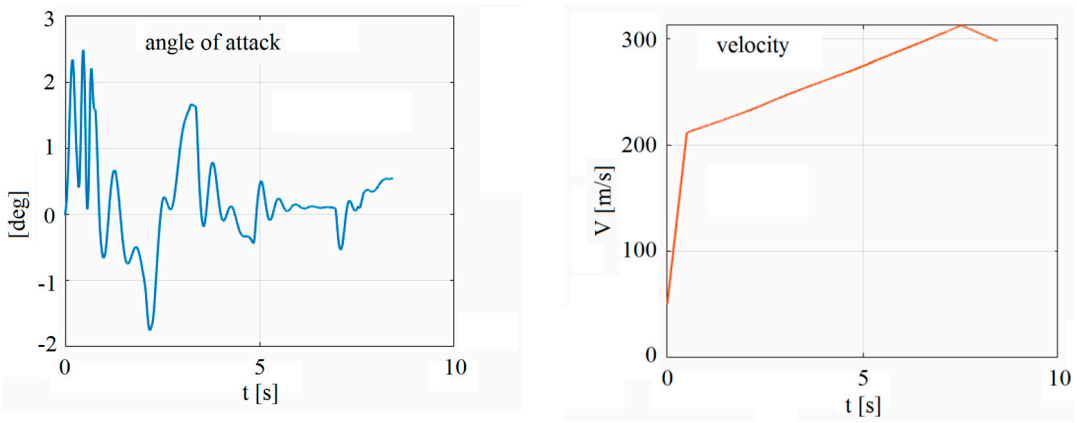

(**a**) (**b**)

Figure 18. Implemented angle of attack α (**a**) and velocity of the ATGM (**b**) in function of time.

5. Final Conclusions, Direction of Further Studies

An algorithm of a modified LQR method utilizing a Jacobian was developed to control the hypothetical missile. The modified regulator calculates control signals (aerodynamic surface deflection angles and the rocket engine thrust vector resultant) based on data from pseudo-real equations of dynamics. The data (state variables) relating to the flight of the missile, such as flight speed, flight angles, angular velocities and spatial position, enable the correct operation of the proposed algorithm; i.e., they are signals required to determine the control signals, which enable the missile to follow the set trajectory.

Modified LQR system model linearization, i.e., calculating the new state matrix and control matrix values takes place at a lower frequency than that at which the regulator itself operates. The linearization frequency is 10 Hz, while the regulator operating frequency is 1000 Hz. This enables the autopilot computing unit to save a significant amount of power, while simultaneously preserving sufficient conformity of the dynamics model with the pseudo-real object in the area of a given operating point. The conducted simulations indicate that the discussed model works correctly. The ATGM follows a set trajectory and precisely hits a moving ground target.

The application of the time-varying elements of the $\mathbf{J}(t)$ and $\mathbf{B}(t)$ matrices allowed the linearization of the flight equations of dynamics in the course of subsequent integration steps. Thus, the dynamic nature of the flight equations was preserved. In practice, a Jacobian in the form of a matrix $\mathbf{J}$ is used—with the matrix containing partial derivatives. This results in the possibility of controlling a highly non-linear and non-stationary object via an LQR.

This article demonstrates that using a linear-quadratic regulator (LQR) for controlling an anti-tank guided missile is possible and enables the smooth maneuvering of the missile, until it reaches a ground target. In addition, this method will be applied in further research work on using a state observer (in the case of a lack of access to all state variables) or an extended Kalman filter, especially in the conditions of random ATGM disturbances.

Author Contributions: Conceptualization, Ł.N. (Łukasz Nocoń), M.G., P.S. and Z.K.; methodology, Ł.N. (Łukasz Nocoń) and Z.K.; software, Ł.N. (Łukasz Nocoń), M.G., P.S. and Z.K.; validation, Ł.N. (Łukasz Nocoń), M.G., P.S., Z.K. and Ł.N. (Łukasz Nowakowski); formal analysis, investigation and resources, Ł.N. (Łukasz Nocoń), M.G., P.S. and Z.K.; data curation, Ł.N. (Łukasz Nocoń), M.G., P.S., Z.K. and Ł.N. (Łukasz Nowakowski); writing—original draft preparation, writing—review and editing and visualization, Ł.N. (Łukasz Nocoń), M.G. and P.S. All authors have read and agreed to the published version of the manuscript.

Funding: This research was funded by the National Center for Research and Development of Poland, grant number DOB-2P/03/04/2018.

Conflicts of Interest: The authors declare no conflict of interest.

References

1. Fu, Z.; Dai, Y.; Zhang, K. Research Progress on Design Methods for Missile Integrated Guidance and Control. In Proceedings of the 2017 International Conference on Automation, Control and Robots, Wuhan, China, 22–24 December 2017.
2. Menon, P.K.; Ohlmeyer, E.J. Integrated Design of agile Missile Guidance and Autopilot Systems. *Control Eng. Pract.* **2001**, *9*, 1095–1106. [CrossRef]
3. Khamis, A.; Naidu, D.S.; Kamel, A.M. Nonlinear Optimal Tracking for Missile Gimbaled Seeker Using Finite-Horizon State Dependent Riccati Equation. *Int. J. Electron. Telecommun.* **2014**, *60*, 165–171. [CrossRef]
4. Das, S.; Halder, K.; Gupta, A. LQR based improved discrete PID controller design via optimum selection of weighting matrices using fractional order integral performance index. *Appl. Math. Model.* **2013**, *37*, 4253–4268. [CrossRef]
5. Rojas, J.H.C.; Serrezuela, R.R.; López, J.A.Q.; Perdomo, K.L.R. LQR Hybrid Approach Control of a Robotic Arm Two Degrees of Freedom. *Int. J. Appl. Eng. Res.* **2016**, *11*, 9221–9228.
6. Isa, A.I.; Hamza, M.F.; Muhammad, M. Hybrid Fuzzy Control of Nonlinear Inverted Pendulum System. *Bayero J. Eng. Technol.* **2019**, *14*, 200–208.
7. Yazdanpanah, R.; Mahjoob, M.J.; Abbasi, E. Fuzzy LQR Controller for Heading Control of an Unmanned Surface Vessel. In Proceedings of the International Conference in Electrical and Electronics Engineering, San Francisco, CA, USA, 23–25 October 2013.
8. Bhangal, N.S. Design and Performance of LQR and LQR based Fuzzy Controller for Double Inverted Pendulum System. *J. Image Graph.* **2013**, *1*, 143–146. [CrossRef]
9. Balandat, M.; Zhang, W.; Abate, A. On Infinite Switched LQR Problems with State and Control Constraints. *Syst. Control Lett.* **2012**, *61*, 464–471. [CrossRef]
10. Zhang, W. Controller Synthesis for Switched Systems Using Approximate Dynamic Programming. Ph.D. Thesis, ECE Department, Purdue University, West Lafayette, IN, USA, 2009.
11. Bużantowicz, W. Tuning of a Linear-Quadratic Stabilization System for an Anti-Aircraft Missile. *Aerospace* **2021**, *8*, 48. [CrossRef]
12. Dinesh, K.; Narendra Kumar, D.; Vijaychandra, J.; Sesha Sai, B.; Vedaprakash, K.; Srinivasa Rao, K. A Review on Cascaded Linear Quadratic Regulator Control of Roll Autopilot Missile. *Ssrn Electron. J.* **2021**, *1*, 88–97.
13. Zheng, X.; Yang, S.C.; Zhang, K.Q. Design and Simulation of Trajectory Tracking Guidance Law Based on LQR for Target Missile. *Mater. Sci. Eng.* **2018**, *435*, 012021. [CrossRef]
14. Vinodh, K.E.; Jovitha, J. Algebraic Riccati equation based Q and R matrices selection algorithm for optimal LQR applied to tracking control of 3rd order magnetic levitation system. *Arch. Electr. Eng.* **2016**, *65*, 151–168.
15. Bużantowicz, W. A sliding mode controller design for a missile autopilot system. *J. Theor. Appl. Mech.* **2020**, *58*, 169–182. [CrossRef]
16. Vinodh, K.E.; Raaja, G.S. A new algebraic LQR weight selection algorithm for tracking control of 2 DoF torsion system. *Arch. Electr. Eng.* **2017**, *66*, 55–75.
17. Holzhuter, T. LQG approach for the high-precision track control of ships. *IEE Proc. Control Theory Appl.* **1997**, *144*, 121–127. [CrossRef]
18. Chatys, R.; Panich, A.; Jurecki, R.S.; Kleinhofs, M. Composite materials having a layer structure of 'sandwich' construction as above used in car safety bumpers. In Proceedings of the 2018 11th International Science and Technical Conference Automotive Safety, Casta Papiernicka, Slovakia, 18–20 April 2018; pp. 1–8.
19. Bużantowicz, W.; Pietrasieński, J. Dual-control missile guidance: A simulation study. *J. Theor. Appl. Mech.* **2018**, *56*, 727–739. [CrossRef]
20. Nocoń, Ł.; Koruba, Z. Modification of control actuation systems of ATGM. In Proceedings of the 23rd International Conference on Engineering Mechanics, Svratka, Czech Republic, 15–18 May 2017; pp. 714–717.
21. Koruba, Z.; Nocoń, Ł. Optimal Compensator for Anti-Ship Missile with Vectorization of Engine Thrust. *Appl. Mech. Mater.* **2016**, *817*, 279–288.
22. Chatys, R. Investigation of the Effect of Distribution of the Static Strength on the Fatigue Failure of a Layered Composite by Using the Markov Chains Theory. *Mech. Compos. Mater.* **2013**, *48*, 629–638. [CrossRef]
23. Gapiński, D.; Stefański, K. A control of modified optical scanning and tracking head to detection and tracking air targets. *Solid State Phenom.* **2014**, *210*, 145–155. [CrossRef]
24. Gapinski, D.; Koruba, Z.; Krzysztofik, I. The model of dynamics and control of modified optical scanning seeker in anti-aircraft rocket missile. *Mech. Syst. Signal Process.* **2014**, *45*, 433–447. [CrossRef]
25. Nocoń, Ł.; Stefański, K. Impact of Controller Performance on the Process of Guiding an Armour-Piercing Missile onto a Ground-Based Target. *Probl. Mechatron. Armament Aviat. Saf. Eng.* **2016**, *7*, 67–84. [CrossRef]
26. Baranowski, L. Effect of the mathematical model and integration step on the accuracy of the results of computation of artillery projectile flight parameters. *Bull. Pol. Acad. Sci. Tech. Sci.* **2013**, *61*, 475–484. [CrossRef]
27. Koruba, Z.; Osiecki, J.W. *Construction, Dynamics and Navigation of Close-Range Missiles—Part 1*; University Course Book No. 348; Kielce University of Technology Publishing House: Kielce, Poland, 1999.
28. Matlab Lqr Function Documentation. Available online: https://www.mathworks.com/help/control/ref/lqr.html (accessed on 1 December 2021).

29. Tewari, A. *Modern Control Design with Matlab and Simulink*; John Wiley & Sons: Chichester, UK, 2002.
30. Bryson, A.E.; Ho, Y.C. *Applied Optimal Control: Optimization, Estimation, and Control*, 1st ed.; Routledge: Boca Raton, FL, USA, 1975; pp. 366–367.